

# Pseudo–Evolution of Galaxies in $\Lambda$ CDM Cosmology

Vasanth Balakrishna Subramani<sup>1</sup>★†, Pavel Kroupa<sup>1,3</sup>, Hossein Shenavar<sup>2</sup>, Vyoma Muralidhara<sup>4</sup>

<sup>1</sup>*Helmholtz-Institut für Strahlen- und Kernphysik (HISKP), Universität Bonn, Nussallee 14-16, D-53115 Bonn, Germany*

<sup>2</sup>*Department of Physics, Ferdowsi University of Mashhad, P.O. Box 1436, Mashhad, Iran*

<sup>3</sup>*Charles University in Prague, Faculty of Mathematics and Physics, Astronomical Institute, Holešovičkách 2, 180 00 Praha 8, Czech Republic*

<sup>4</sup>*Argelander-Institut für Astronomie, Universität Bonn, Auf dem Hügel 71, 53121 Bonn, Germany*

accepted July 2019

## ABSTRACT

Our knowledge about galaxy evolution comes from transforming observed galaxy properties at different redshifts to co-moving physical scales. This transformation depends on using a cosmological model. Here the effects of unintentional mixing of two different cosmological models on the size evolution of galaxies is studied. As a gedanken experiment, a galaxy of fixed proper size and luminosity is moved across different redshifts. The apparent size of this galaxy is then interpreted with a cosmological model presumed by the observer, which is different compared to the cosmology exhibited by the Universe. In such a case, a spurious size evolution of the galaxy is observed. A galaxy behaving according to the  $R_h = ct$  and Neumann’s cosmology, when interpreted with the  $\Lambda$ CDM cosmological model, shows an increase in size by a factor of 1.1 and 1.3 from  $z = 7.5$  to  $z \approx 0$ , respectively. The apparent size of a galaxy in a static Euclidean cosmology, when interpreted in the  $\Lambda$ CDM model, shows a factor of 23.8 increase in size between  $z = 7.5$  to  $z \approx 0$ . This is in close agreement with the observational data with a size increase of a factor of 6.8 between  $z = 3.2$  to  $z \approx 0$ . Furthermore, using the apparent size data, it is shown that the difference between the derived proper sizes in  $R_h = ct$ , Neumann’s and  $\Lambda$ CDM cosmological models are minimal.

**Key words:** galaxies: evolution – galaxies: distances and redshifts – cosmology: theory – cosmological parameters – gravitation

## 1 INTRODUCTION

Galaxies are born and evolve subject to cosmological boundary conditions. At the same time, the physical parameters describing a galaxy at any cosmological epoch can only be determined by applying a pre-supposed cosmological model in the interpretation of the observed, apparent parameters. Our knowledge of cosmology and our knowledge of galaxy formation and evolution are thus interrelated. With this contribution we aim to elucidate this issue, raising the question how reliable our understanding of galaxy evolution is, given that some doubts on the validity of the standard  $\Lambda$ CDM cosmology have been raised (see below).

There are a number of geometrical tests – Hubble diagrams (Laviollette 1986; Schade, Barrientos & López-Cruz 1997; Marosi 2013), Tolman surface brightness tests (Lubin & Sandage 2001; Andrews 2006; Lerner 2006; Lerner et al. 2014), angular size tests (Kapahi 1987; Kellermann 1993; López-Corredoira 2010) – to deduce the correct cosmological model. However, almost all these tests are affected by the unknown physical size evolution of galaxies at high redshift. The observationally deduced proper sizes of

galaxies are in addition six times smaller at  $z = 3.2$  than at  $z = 0$  (López-Corredoira 2010). Such a strong size evolution is poorly understood despite numerous attempted explanations relying on e.g. higher densities (Mo, Mao & White 1998; Ferguson et al., 2004; Trujillo et al., 2006), luminosity evolution (Shen et al. 2003), mergers (Trujillo et al. 2006, 2007), or massive outflows due to quasar feedback (Fan, Lapi, De Zotti & Danese 2008). However, the static Euclidean cosmological model fits the data without any necessity of a size evolution of a galaxy (Lerner 2018).

In addition, the angular size test is also used to constrain the various parameters of cosmological models. Lerner et al. (2014) argue that the observed UV surface brightness of galaxies are inconsistent with an expanding Universe but are consistent with a static Euclidean Universe. This application of the Tolman test on the data leaves the physical origin of the observed galaxy redshift unaccounted for. Wei, Wu & Melia (2015) used the galaxy angular size with redshift to study  $\Lambda$ CDM and  $R_h = ct$  cosmological models. These authors have shown that the best-fitting values of the  $\Lambda$ CDM model occur when  $(\Omega_m, H_0) = (0.50, 73.9_{-9.5}^{+10.6} \text{ km s}^{-1} \text{ Mpc}^{-1})$ . This estimated matter share of the Universe is significantly different from the concordance parameter  $\Omega_m \approx 0.3$  derived by the Planck Collaboration et al. (2016). It is also shown that, although both models appear to fit the data based on their  $\chi^2$ , Bayes Information Criterion (as the selection tool) favours  $R_h = ct$  over  $\Lambda$ CDM with a

★ Contact e-mail: bs.vasanth@gmail.com, pkroupa@uni-bonn.de

† Present address: Helmholtz-Institut für Strahlen- und Kernphysik (HISKP), Universität Bonn, Nussallee 14-16, D-53115 Bonn, Germany

likelihood of 86% versus 14%. Also prior studies have shown that unless one presumes a surprisingly large increase in the size of elliptical and disk galaxies (a growth factor of  $\approx 6$  from  $z \approx 3$  to 0) they do not match these models. Therefore [Wei et al. \(2015\)](#) have concluded that because  $\Lambda$ CDM cosmology fits the data as well as  $R_h = ct$  model, the large growth rate might be due to some other astrophysical phenomena such as mergers and/or selection effects rather than an incorrectly applied expansion. For example, [Suess et al. \(2019\)](#) find that the half-light radius grows much more rapidly with time than the half-mass radius which shows little evolution over the redshift range  $z \approx 2.5$  to 1.5.

Numerous studies have tried to implement ultra – compact radio sources as a better standard rod. As reasoned by [Kellermann \(1993\)](#) and [Gurvits, Kellermann & Frey \(1999\)](#) the underlying physics of these ultra–compact radio sources is mostly governed by a limited number of physical parameters, such as the mass of the central black hole, the accretion rate. Thus compact radio sources are less prone to evolutionary effects than extended radio sources. [Zhu, Fujimoto & He \(2004\)](#) used the same data as [Gurvits et al. \(1999\)](#) of the compact radio sources and X-ray gas mass fractions of galaxy clusters to determine the equation of state of dark energy. They have found that in a flat universe, the equation of state of dark energy is bounded as  $-2.22 < w_x < -0.62$  at 95.4 % confidence level. This represents a nontrivial lower bound on  $w_x$ .

[López-Corredoira \(2010\)](#) and [Pashchenko & Vitriřchak \(2011\)](#) have questioned the validity of the ultra-compact radio sources as standard rods. Using the ultra-compact radio sources, [Kellermann \(1993\)](#) suggests the Einstein-de Sitter model to be a more viable model, whereas [Jackson & Dodgson \(1997\)](#), using a much larger sample with a very different measure of angular size, and at a lower frequency, state it is not compatible with Einstein-de Sitter but with a solution  $\Omega_m = 0.2$  and  $\Omega_\Lambda = 0.8$ . [Jackson \(2004\)](#) and [Jackson & Jannetta \(2006\)](#) update and confirm this result using an expanded data set. [Pashchenko & Vitriřchak \(2011\)](#) suggest that the resolution of the ground based VLBI data and their dependence on the flux has an effect on the luminosity-linear size correlation. They conclude that it is not feasible to use ultra-compact radio sources as standard rods, a criticism challenged by [Jackson \(2012\)](#).

Although, baryonic acoustic oscillations in cosmic microwave background radiation or large scale structure are considered as the standard rod for cosmic expansion ([Rassat & Refregier 2012](#)), it does not have any relevance on the standard rod in the context of galaxy size evolution. Dust emission at cosmological distances may significantly affect the CMB ([Vavrycuk 2017](#)) such that the Planck solution to the  $\Lambda$ CDM model may need to be revised, and significant problems of the  $\Lambda$ CDM model have been documented on all scales ([Kroupa et al. 2010](#); [Peebles & Nusser 2010](#); [Famaey & McGaugh 2012](#); [Kroupa 2012, 2015](#); [Haslbauer et al. 2019](#)). The significant tension between the locally-measured-Hubble-Lemaitre constant and the value predicted using the standard  $\Lambda$ CDM model and Planck satellite measurements of the CMB is becoming an unsurmountable problem ([Riess et al. 2019](#)). Thus the  $\Lambda$ CDM model may not be the correct description of the Universe ([Kroupa 2012](#); [Lerner et al. 2014](#); [Lerner 2018](#); [Melia & López-Corredoira 2018](#)).

The current circumstances thus make it conducive to perform a gedanken experiment by taking a hypothetical standard rod of, for example, 50 kpc in order to study the dependence of the inferred apparent size on the cosmological model. For this a theoretical galaxy of radius 25 kpc is moved through different redshifts and its apparent size is interpreted via  $R_h = ct$ , Neumann and  $\Lambda$ CDM cosmological models. This enables to quantify the actual depen-

dence of the apparent size on the cosmological model independent of any size evolution mechanism. As an example, using the data of apparent size and redshift from table 1 of [Lerner \(2018\)](#), the cosmology dependence on interpreting the proper size and luminosity from their apparent measurements is illustrated here. Furthermore, the effect of using a particular pre-supposed cosmological model to study the apparent size of a galaxy that is in reality immersed in another cosmological model is demonstrated. A spurious size evolution of galaxies is observed.

The outline of this paper is as follows: Section 2 develops the Hubble-Lemaitre parameter in different cosmological models. Section 3 compares the angular diameter distance and luminosity distance in different cosmologies and subsequently its effect on the deduced apparent radius and apparent magnitude of a theoretical galaxy. Using data from table 1 of [Lerner \(2018\)](#) the dependence of cosmology in deducing the proper size of galaxies is exemplified in Section 4. In Section 5 and Section 6, the pseudo-evolution of galaxies with redshift in an expanding and non-expanding universe is introduced, respectively. Section 7 concludes with results and future prospects. The Appendix gives a brief introduction to cosmological perturbation theory used to arrive at Neumann’s cosmological model.

## 2 HUBBLE’S PARAMETER

The Hubble-Lemaitre (H-L) parameter,  $H$ , forms the crux of any expanding model of the Universe. It is essential to arrive at the notion of distance, and further to derive apparent magnitude and apparent size. Hence, in this section a brief introduction to the H-L parameter is given for Neumann,  $R_h = ct$  and  $\Lambda$ CDM cosmological models because this is not available in the current literature. The Neumann cosmological model is based on using the Neumann boundary condition on Eq. 25 derived from cosmological perturbation theory in the Appendix ([Shenavar 2016](#)). In Neumann’s model, the Friedmann metric is used as the background metric along with a scalar perturbation. In order to arrive at the H-L parameter in Neumann’s model it is necessary to first determine the  ${}^lG_{00}$  component of Einstein’s field equation for the background metric, which is given in Eq. 23 in the Appendix. Taking the  ${}^lG_{00}$  component in Eq. 23 and substituting for  $\Phi$  using Eq. 26 and collecting the terms proportional to  $c_1$  to the right hand side of terms obtains

$$\frac{12\Psi H^2}{R^4} + \frac{2\nabla^2\Psi}{R^4} = 4\pi R^2 G\delta T_0^0 + \frac{6c_1 H^2}{R^2}. \quad (1)$$

Now, taking the terms proportional to  $c_1$  and adding them to the  ${}^bG_{00}$  component of Einstein’s field Eq. 22, the non-standard Friedmann’s equation results,

$$3H^2 = 8\pi G\rho + \frac{6c_1 H^2}{R^2}, \quad (2)$$

along with the constant  $c_1$  term contributing to the energy density. Here the additional term with  $c_1$  in Eq. 2 is rearranged to get  $8\pi G\rho_{c_1}$ , where  $\rho_{c_1}$  referred to as the Neumann term. The  $\rho_{c_1}$  also contributes to the overall energy density along with the conventional energy density  $\rho$ , where  $\rho$  is composed of baryonic matter density,  $\rho_m$ , and radiation density,  $\rho_r$ . The interpretation for the constant  $c_1$  is still an open question. For an experimental determination of the value of  $c_1$  using strong lensing systems see [Shenavar \(2016\)](#). This derivation is different from eq. 57 in the appendix of [Shenavar \(2016\)](#) since the correct expression of  ${}^lG_{00}$  from eq. 7.38 in [Mukhanov \(2005\)](#) is used, and  $\Phi = \Psi - c_1$  is substituted instead of  $\Psi$  as given in eq. 20 of [Shenavar \(2016\)](#). Therefore, this

derivation also serves as an erratum for the derivation of eq. 57 of Shenavar (2016).

The energy densities at time  $t$  can be written into the more favoured dimensionless density parameters

$$\Omega_i \equiv \frac{8\pi G\rho_i(t)}{3H^2(t)}, \quad (3)$$

and

$$\Omega_k \equiv -\frac{k}{H^2(t)R^2(t)}, \quad (4)$$

where  $k = -1, 0$  and  $1$  for a hyperbolic, flat and closed universe, respectively.

Writing the Friedmann Eq. 2 in terms of  $\Omega_{0,i}$ ,

$$H^2(t) = H_0 \left( \frac{\Omega_{0,m}}{a^3} + \frac{\Omega_{0,r}}{a^4} + \frac{\Omega_{0,k}}{a^2} + \Omega_{0,c1} \frac{H}{H_0} \right), \quad (5)$$

in which  $\Omega_{0,i}$  is the  $i^{\text{th}}$  density parameter at the present time  $t_0$ , while

$$a(t) \equiv \frac{R(t)}{R_0} = (1+z)^{-1}, \quad (6)$$

is the normalized scale factor. Here  $\Omega_{0,m}$ ,  $\Omega_{0,r}$ ,  $\Omega_{0,k}$  and  $\Omega_{0,c1}$  are the baryonic matter, radiation, curvature and Neumann densities of the universe, respectively. The curvature density parameter is set at zero assuming the universe to be flat, and the value of the Neumann term is obtained using the flatness condition  $\Omega_{tot} = \sum_i \Omega_i(t) = 1$ . Here,  $\Omega_{0,m}$  represents only the baryonic matter, not inclusive of dark matter, unlike in the  $\Lambda$ CDM cosmological model, to give the Neumann cosmological model parametric freedom. By solving the quadratic Eq. 5 and taking only the positive solution<sup>1</sup> for the square root we get the Neumann H-L parameter,

$$H_{Neu}(t) = \frac{H_0}{2} \left( \Omega_{0,c1} + \sqrt{\Omega_{0,c1}^2 + 4 \left( \frac{\Omega_{0,k}}{a^2} + \frac{\Omega_{0,m}}{a^3} + \frac{\Omega_{0,r}}{a^4} \right)} \right). \quad (7)$$

In the  $R_h = ct$  cosmological model the universe expands with the constant velocity of speed of light  $c$  (Melia & Shevchuk 2012). Therefore, in this case the scale factor is  $a = ct$ , and the H-L parameter,

$$H = \frac{\dot{a}}{a},$$

becomes  $H = 1/t$ . Substituting for  $t$  via the expression  $1+z = \frac{a(t_0)}{a(t)} = \frac{t_0}{t}$ , where  $t$  and  $t_0$  are emission and observation time, respectively, gives the H-L parameter in the  $R_h = ct$  cosmological model as (Wei et al. 2017; Yennapureddy & Melia 2017)

$$H_{R_h} = H_0(1+z). \quad (8)$$

Here  $H_0$  is the current value of the H-L parameter, and it is also the only sole free parameter.

The H-L parameter in the  $\Lambda$ CDM model is given by

$$H_{\Lambda\text{CDM}}^2(t) = H_0^2 \left( \frac{\Omega_{0,k}}{a^2} + \frac{\Omega_{0,m}}{a^3} + \frac{\Omega_{0,r}}{a^4} + \Omega_{0,\Lambda} \right), \quad (9)$$

where  $\Omega_{0,m}$ ,  $\Omega_{0,r}$ ,  $\Omega_{0,k}$ , and  $\Omega_{0,\Lambda} \equiv \frac{\Lambda}{3H_0^2}$  are the present-day matter (including the dark matter), radiation, curvature and dark energy density parameters, respectively, with  $\Lambda$  being a cosmological constant associated with dark energy. The value of  $H_{+\Lambda\text{CDM}}$  or  $H_{-\Lambda\text{CDM}}$  gives an expanding or contracting universe, respectively. Throughout this paper  $H_+$  and a flat universe is assumed for the Neumann,

<sup>1</sup> The negative sign corresponds to a contracting universe.

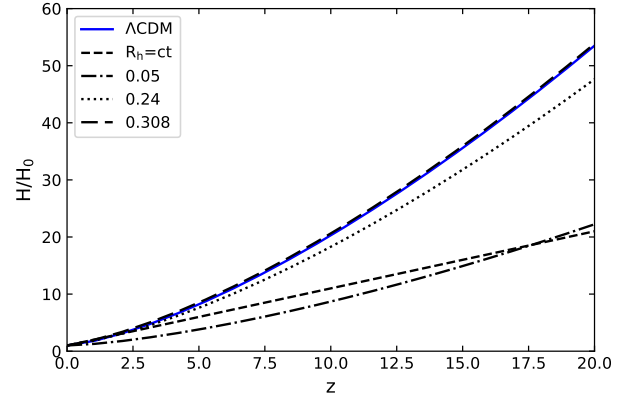


**Figure 1.** The blue curve shows the H-L parameter with respect to redshift for the  $\Lambda$ CDM cosmology. The Neumann cosmology is shown with different baryonic matter densities and the H-L parameter for the  $R_h = ct$  model is the linear relation shown as a dashed straight line. This figure is normalized to the current value of the H-L parameter as obtained by the recent Planck Collaboration et al. (2016).

$R_h = ct$  and  $\Lambda$ CDM cosmological models (Planck Collaboration et al. 2016). In Fig 1 the evolution of H-L parameter with respect to redshift  $z$  is compared for all the models. The Neumann model is also plotted for different baryonic matter densities, one notices that for both the Neumann and  $\Lambda$ CDM models, the H-L parameter coincides for  $\Omega_m = 0.308$ ,  $\Omega_r = 5 \times 10^{-5}$  and  $\Omega_\Lambda = 0.691$ , which are the values from the recent Planck analysis (Planck Collaboration et al. 2016). In Neumann's model  $\Omega_m$  is interpreted as only the baryonic density, whereas in the  $\Lambda$ CDM it is total matter density including dark matter.

It also noted that the H-L parameter for the  $R_h = ct$  cosmology follows a straight line as it does not depend on any components of the cosmological fluid. Although it looks similar to Milne cosmology it is distinct from it by having a non-zero energy density.

### 3 A POTPOURRI OF COSMOLOGIES

Any object at redshift  $z$  and with a physical co-moving (proper) diameter  $D$  [kpc] and absolute magnitude  $M$  will have a diameter in radians on the sky of

$$\delta\theta = \frac{D}{D_A(z)} \quad (10)$$

and an apparent magnitude of

$$m = M + 5 \log_{10} \frac{D_L}{10}. \quad (11)$$

The deduction of the proper diameter and the absolute magnitude of the object in the sky by using Eq.10 and Eq. 11 depends on the cosmological model through the angular diameter distance  $D_A$  and luminosity distance  $D_L$ , respectively.

The general definition of the luminosity distance and the angular distance in any cosmological model is

$$D_L = c(1+z) \int_0^z \frac{dz'}{H(z')} \text{ Mpc}, \quad (12)$$

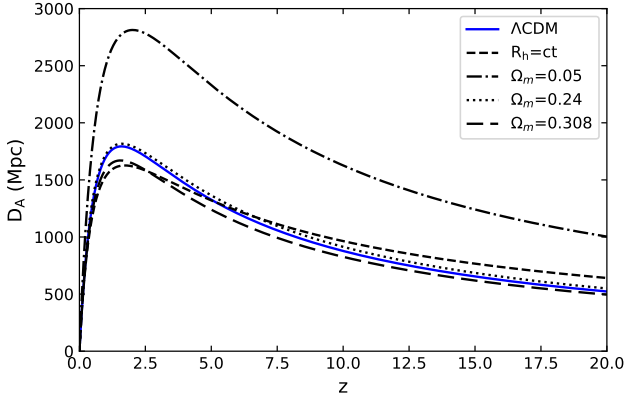


**Figure 2.** The angular diameter distance with respect to redshift for  $\Lambda$ CDM,  $R_h = ct$  and Neumann's cosmology. Symbols are as in Fig. 1. This figure also serves as an erratum for the fig. 8 in Shenavar & Javidan (2018).

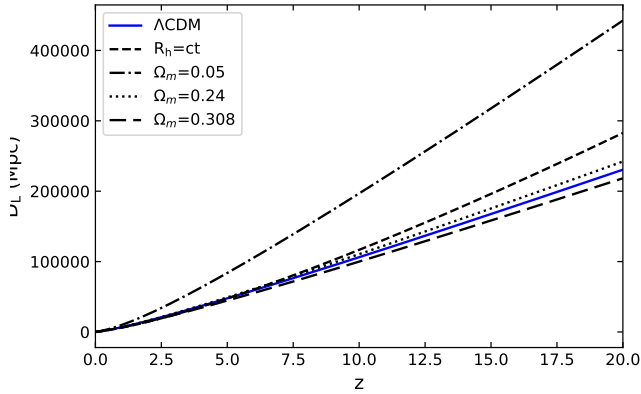


**Figure 3.** The luminosity distance with respect to redshift for  $\Lambda$ CDM,  $R_h = ct$  and Neumann's cosmology. This figure also serves as an erratum for the fig. 7 in Shenavar & Javidan (2018).

and

$$D_A = \frac{c}{1+z} \int_0^z \frac{dz'}{H(z')} \text{ Mpc}, \quad (13)$$

respectively. Therefore the distances in  $\Lambda$ CDM<sup>2</sup>,  $R_h = ct$  and Neumann's cosmological models are obtained by inserting their respective definitions of the H-L parameter. As a representative example, for the  $R_h = ct$  cosmological model (Wei et al. 2015)

$$D_A = \frac{c}{H_0} \frac{\ln(1+z)}{1+z}, \quad (14)$$

by inserting  $H_{R_h}$  in Eq. 13 with  $H_0$  being the current value of the H-L parameter.

Figures 2 and 3 show the angular diameter distance and luminosity distance for  $\Lambda$ CDM,  $R_h = ct$ , and Neumann's cosmological models for different baryonic mass densities. As evident in Fig. 2,

<sup>2</sup> From here on we refer to the  $\Lambda$ CDM model "as the standard cosmological model with the Planck Collaboration et al. (2016) data."

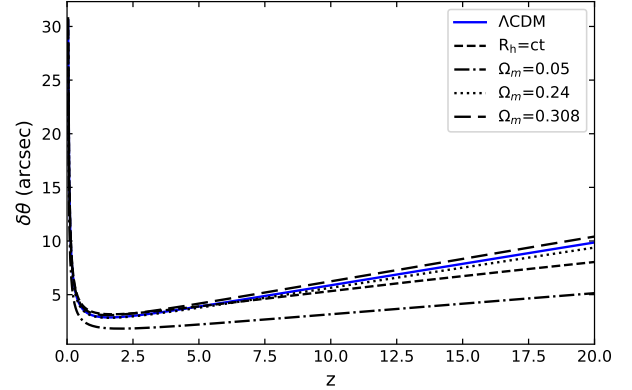


**Figure 4.** The apparent radius of a galaxy with a proper radius of 25 kpc in the  $\Lambda$ CDM, the  $R_h = ct$  and the Neumann cosmological models.

all the three cosmological models show a cosmological lensing effect, that is, the apparent size of an object might seem to increase for distances approximately farther than  $z = 1$  (see Fig. 4). This is the consequence of expanding universe models. Furthermore, Fig. 2 shows that for a given redshift the same object is closer in Neumann's model with baryonic matter density  $\Omega_m = 0.308$  compared to the  $\Lambda$ CDM model, which is also modelled for a total matter density (baryonic matter and dark matter) of  $\Omega_m = 0.308$ . For  $R_h = ct$  and  $\Lambda$ CDM cosmological models the distance to the same object differ only in the peak and for later redshifts. On the other hand, the distances in the Neumann model increases with decreasing baryonic matter density.

In Figure 3, the luminosity distance for the same object at a given redshift is inferred to be larger in  $R_h = ct$  compared to  $\Lambda$ CDM and Neumann's cosmological model with  $\Omega_m > 0.2$ . The luminosity distance for both the  $\Lambda$ CDM and  $R_h = ct$  models are distinguishable only at higher redshifts beyond  $z = 5$ . For the Neumann cosmological model the inferred luminosity distance of an object looks closer for a universe with higher baryonic matter density. The curve with same baryonic matter density as the Planck solution seems to be nearer in the Neumann model than in  $R_h = ct$  and  $\Lambda$ CDM cosmological models. The consequence of these differences in the angular diameter distance and luminosity distance can lead to deducing a different proper size and absolute magnitude using the observed apparent size and apparent magnitude in different cosmological models.

This problem is illustrated by taking a galaxy of fixed proper radius of 25 kpc and fixed absolute magnitude  $M_V = -21.5$  (apparent magnitude of the Andromeda galaxy) in the photometric V-band (Ribas et al. 2005), and moving it through different redshifts, while observing the differences in the apparent measurements of the galaxies by different cosmological models.

In Figure 4, the deduced apparent radius in  $\Lambda$ CDM and the  $R_h = ct$  models are smaller than in Neumann's cosmological model with  $\Omega_m = 0.308$  for a given redshift of a galaxy with 25 kpc radius. The apparent size also decreases with decreasing baryonic matter densities for the Neumann cosmological model. It is also pertinent to note that if the universe behaved with a different cosmological model, suppose with the Neumann cosmological model with  $\Omega_m = 0.05$ , then a galaxy at  $z = 10$  will appear to be bigger from the perspective of  $\Lambda$ CDM and  $R_h = ct$  cosmological models.

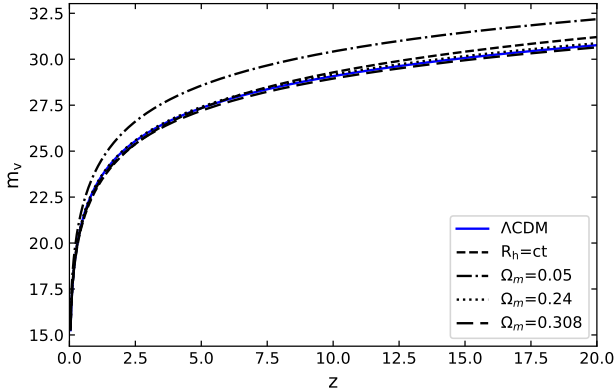


**Figure 5.** The apparent magnitude of the Andromeda galaxy with absolute V-band magnitude  $M = -21.5$  in all the three cosmological models.

Figure 5 depicts the apparent magnitude of the Andromeda galaxy as interpreted by the different cosmological models. The Andromeda galaxy at very high redshift appears to be dimmer (the value of  $m$  increasing) in  $\Lambda$ CDM and  $R_h = ct$  models as compared to Neumann’s cosmological model with  $\Omega_m = 0.308$ . It also appears dimmer with decreasing baryonic matter density in Neumann’s cosmological model.

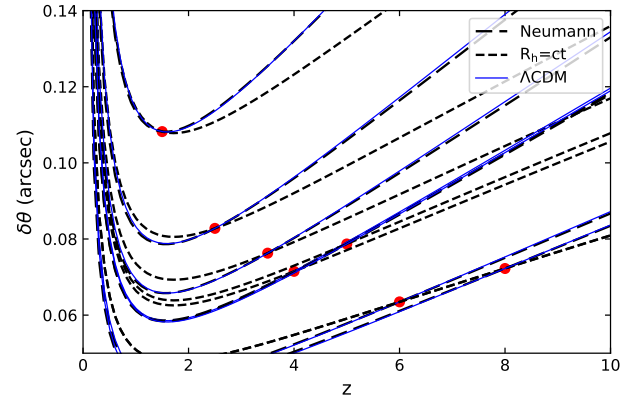
#### 4 AN EXAMPLE

In this section, the cosmological dependence on interpreting the proper size is studied by taking the apparent radius<sup>3</sup> of the galaxies given in table 1. of Lerner (2018).

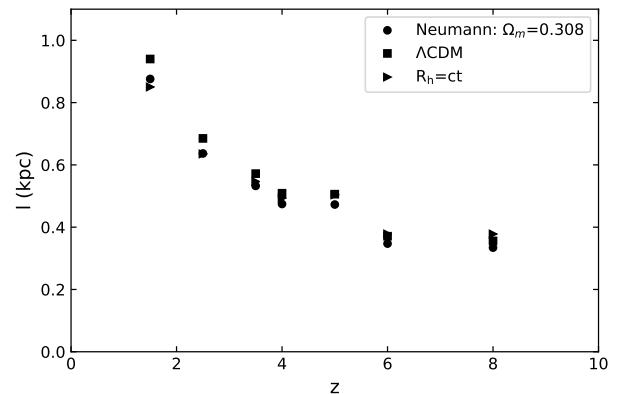
In Figure 6, the apparent sizes of the galaxies are fitted with their respective deduced proper sizes from the  $\Lambda$ CDM,  $R_h = ct$  and Neumann’s cosmological model. Figure 6 shows the deduced proper size curves for each data point in different models.

Figure 7 depicts the deduced proper size for individual data points by the different cosmological models. In the lower redshift region upto  $z = 4$  the  $\Lambda$ CDM and Neumann models appear to imply a larger proper size, but the proper size deduced from the  $R_h = ct$  cosmological model dominates at  $z \geq 6$ . Overall the galaxies have increased approximately twice in size from  $z = 8$  to  $z = 1$ . This is a small size evolution in comparison to Trujillo et al. (2006), which concludes a size evolution by a factor of 3 from  $z = 2.5$  to  $z = 0$ . For heavier galaxies Trujillo et al. (2007) conclude an evolution of upto a factor of 4 from  $z = 1.5$  to  $z = 0$  and a factor of 5.5 from  $z = 2.3$  to  $z = 0$ . Other studies Ferguson et al. (2004); Bouwens et al. (2004); López-Corredoira (2010); Trujillo et al. (2004); Wiklind et al. (2008); Noll et al. (2009) suggest a size increase by a factor of approximately 6 from  $z = 3$  to  $z = 0$ . See also Suess et al. (2019) for further discussion of possible biases.

<sup>3</sup> The apparent radius is deduced from the proper radius in column two of table 1 from Lerner (2018) using the  $\Lambda$ CDM cosmological model.



**Figure 6.** The curves through each data point (Lerner 2018) depict the deduced proper radius (see also Fig. 7) of the apparent radius of galaxies by using  $\Lambda$ CDM,  $R_h = ct$  and Neumann ( $\Omega_m = 0.308$ ) cosmological models. The proper sizes are derived by using the relationship between the apparent size, proper size and distance from the respective cosmological model given by Eq. 10. The different curves show that for the same data point the deduced proper size depends on the cosmological model the observer chooses to use.



**Figure 7.** The deduced proper radius from the apparent radius of the galaxies shown in Fig. 6. Here all the cosmologies show a size evolution from the past to present, however the galaxies inflate only approximately by a factor of two between  $z = 8$  and  $z = 0$ , which is significantly smaller compared to the factor of 6 between  $z = 3$  to  $z = 0$  reported by Ferguson et al. (2004); Bouwens et al. (2004); López-Corredoira (2010); Trujillo et al. (2004); Wiklind et al. (2008); Noll et al. (2009). Note that the differences in the deduced proper radius in the different expanding cosmological models are minimal.

#### 5 PSEUDO-EVOLUTION IN AN EXPANDING UNIVERSE

In Sec. 4, the effect on the size evolution dependent only on the cosmological model is obtained in Fig. 7. Here the question raised is if there can be a spurious size evolution if the universe does not follow the  $\Lambda$ CDM model? Is an incorrect size evolution deduced due to using an incorrect cosmological model? A possibility of such a fake phenomenon is shown by taking a universe that in reality behaves according to a Neumann or  $R_h = ct$  cosmological model, and

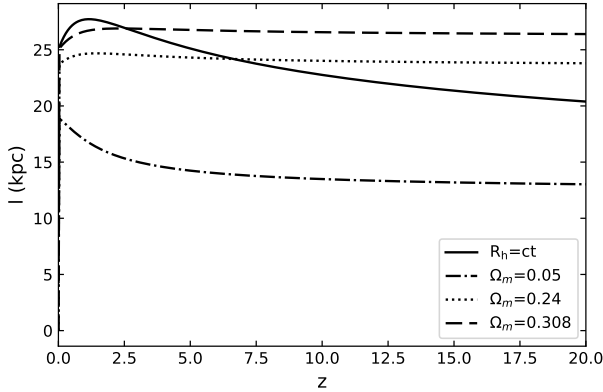


**Figure 8.** The proper size of a theoretical galaxy of fixed radius 25 kpc with redshift. The apparent size in the assumed to be correct Neumann and  $R_h = ct$  universe is interpreted in  $\Lambda$ CDM cosmology.

interpreting the fixed proper size of a galaxy in such a universe with the  $\Lambda$ CDM cosmological model. This is achieved by theoretically generating the apparent size for a galaxy of true proper size of radius 25 kpc in the Neumann and  $R_h = ct$  cosmological model and deducing its proper size using the  $\Lambda$ CDM model.

The relationship between the deduced proper size and theoretically generated apparent size is given by

$$l_{pse} = \delta\theta_{Neu \text{ or } R_h} \times D_{\Lambda\text{CDM}}. \quad (15)$$

Here  $\delta\theta_{Neu \text{ or } R_h}$  is the theoretically generated apparent diameter for a galaxy of (true) proper size of radius 25 kpc in Neumann or  $R_h = ct$  cosmological model. The  $l_{pse}$  is the proper size interpreted for a galaxy in a Neumann or  $R_h = ct$  universe via the angular diameter distance  $D_{\Lambda\text{CDM}}$  of the  $\Lambda$ CDM cosmological model. The apparent size and redshift are the only observed quantity for a universe behaving with a specific cosmology. The calculation here by no means advocates the correctness of any cosmological model. The motivation is rather to perform a gedanken experiment to see the consequences of using two models—one exhibited in reality by the Universe and the other used to interpret this Universe—on the size evolution of a galaxy.

This deduced proper size  $l_{pse}$  using the  $\Lambda$ CDM cosmological model is shown in Figure 8. Here the proper size appears to evolve differently for the galaxy in  $R_h = ct$  cosmology with  $H_0$  as the sole free parameter, and for Neumann’s universe with baryonic matter density of  $\Omega_m = 0.05$ , which is close to the estimated baryonic matter density of Planck solution. This size evolution is unphysical as the galaxy radius is fixed to 25 kpc in both cosmologies. Such a spurious evolution is referred to here as pseudo-evolution. Assuming the Universe is correctly described by the  $R_h = ct$  model, a  $\Lambda$ CDM observer would deduce the galaxy’s radius to evolve from 23.7 kpc at  $z = 7.5$  to 26.3 kpc at  $z \approx 0$ . This is a size evolution by a factor of 1.1 that is purely due to pseudo-evolution. A galaxy in Neumann’s cosmology with  $\Omega_m = 0.05$  has increased in size from 13.7 kpc at  $z = 7.5$  to 18.4 kpc at  $z \approx 0$ , which is an increase in size by a factor of 1.3 due to pseudo-evolution.

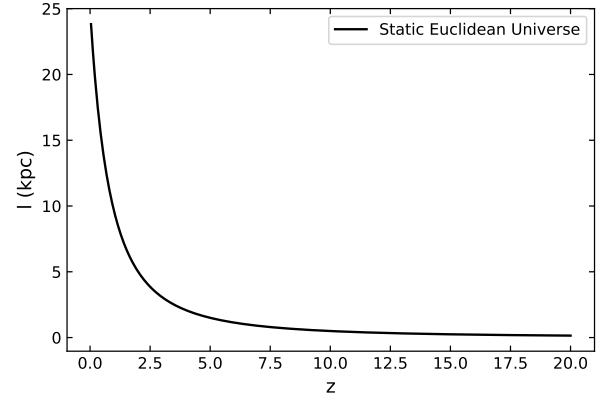


**Figure 9.** The pseudo-evolution of a galaxy of fixed radius, 25 kpc, in static Euclidean model when interpreted via  $\Lambda$ CDM cosmological model.

## 6 PSEUDO-EVOLUTION IN A NON-EXPANDING UNIVERSE

In this section, a galaxy in a non-expanding universe is interpreted in the  $\Lambda$ CDM cosmological model. The distance-redshift relationship for a static universe is (Lerner et al. 2014)

$$D_A(z) = \frac{cz}{H_0}. \quad (16)$$

Note that in this model the redshift is a physical phenomenon that is not related to velocity. Now, taking a galaxy of radius 25 kpc in the static universe, whose apparent size is given by Eq. 10, one can arrive at the pseudo-evolution from Eq. 15, for interpretation via the  $\Lambda$ CDM cosmological model. This is depicted in Fig. 9. The radius of the galaxy appears to increase by a factor of 6.8 between  $z = 3.2$  to  $z \approx 0$ , which is in close agreement with the observed data from the previous studies (López-Corredoira 2010) which state a size evolution of a factor of 6 in the same interval. It is also noted that the size evolution between  $z = 7.5$  to  $z \approx 0$  due to pseudo-evolution is by a factor of 23.81. In any case, we do not argue that the universe is static. This model is taken into account to show that pseudo-evolution between the static and  $\Lambda$ CDM cosmological model does indeed fit the observed data for non-evolving or mildly evolving galaxies.

## 7 CONCLUSION

After a short introduction to  $R_h = ct$ , Neumann’s and  $\Lambda$ CDM cosmological models, a galaxy with a fixed proper radius of 25 kpc and an absolute magnitude  $M_V = -21.5$  is moved in redshift, and its apparent size and apparent magnitude deduced in different cosmological models is noted. This is performed for later comparison of results from individual cosmological models to mixing of different cosmological models leading to pseudo-evolution of a galaxy. Meanwhile, using the apparent measurements from Lerner (2018) as an example, the proper size has been obtained for the above three cosmological models. Fig. 7 shows that these data suggest a growth in the proper radius of galaxies by a factor of about 2 from  $z \approx 8$  to  $z \approx 1$  and that the here considered cosmological models lead to similar results.

In the end, a gedanken experiment on using an observers’

choice of cosmological model to study the Universe which behaves in reality according to a different cosmology is conducted. In this experiment a galaxy of a fixed radius in the  $R_h = ct$  and Neumann's cosmological model is interpreted in the  $\Lambda$ CDM cosmological model. Under such a framework, the galaxy seems to evolve in size by a factor of 1.1 and 1.3 for  $R_h = ct$  and Neumann's cosmological model between  $z = 7.5$  to  $z \approx 0$ , respectively. For a static Euclidean model, the pseudo-evolution is of a factor of 23.8, which closely matches the observed size evolution with a size evolution by a factor of 6.8 between  $z = 3.2$  to  $z \approx 0$  (López-Corredoira 2010). This evolution is not real, it arises from mixing two different cosmological models. The pseudo-evolution in  $R_h = ct$  and Neumann's cosmological models observed with the  $\Lambda$ CDM model alleviates the problem of galaxy size evolution. However, the pseudo-evolution which appears for a true static Euclidean model observed with a  $\Lambda$ CDM model, completely accounts for the problem of galaxy size evolution as pseudo-evolution. In any case, we do not advocate any cosmological model over another. This contribution is to demonstrate the physical effects of presuming a cosmological model for interpretation, when the universe exhibits a different one. Especially, in the context of galaxy size evolution, the previously not documented effect of pseudo-evolution is emphasized as a possibly important issue to consider when galaxy evolution models do not match observational data.

**Acknowledgement:** We thank Eric Lerner for his valuable comments.

## References

- Andrews T. B., 2006, in Lerner E. J., Almeida J. B., eds, American Institute of Physics Conference Series Vol. 822, First Crisis in Cosmology Conference. pp 3–22, doi:10.1063/1.2189118
- Arfken G. B., 2005, *Mathematical methods for physicists*. Elsevier, Boston
- Bardeen J. M., 1980, *Phys. Rev. D*, **22**, 1882
- Bertschinger E., 1995, NASA STI/Recon Technical Report N, 96
- Bouwens R. J., Illingworth G. D., Blakeslee J. P., Broadhurst T. J., Franx M., 2004, *The Astrophysical Journal*, 611, L1
- Carroll S. M., 2014, *Spacetime and Geometry*. Pearson, Harlow
- Famaey B., McGaugh S. S., 2012, *Living Reviews in Relativity*, **15**, 10
- Fan L., Lapi A., De Zotti G., Danese L., 2008, *ApJ*, **689**, L101
- Ferguson H. C., et al., 2004, *ApJ*, **600**, L107
- Gurvits L. I., Kellermann K. I., Frey S., 1999, *A&A*, **342**, 378
- Haslbauer M., Dabringhausen J., Kroupa P., Javanmardi B., Banik I., 2019, arXiv e-prints, p. arXiv:1905.03258
- Jackson J. C., 2004, *J. Cosmology Astropart. Phys.*, 2004, 007
- Jackson J. C., 2012, *MNRAS*, **426**, 779
- Jackson J. C., Dodgson M., 1997, *MNRAS*, **285**, 806
- Jackson J. C., Jannetta A. L., 2006, *J. Cosmology Astropart. Phys.*, 2006, 002
- Javanmardi B., Kroupa P., 2017, *A&A*, **597**, A120
- Javanmardi B., Porciani C., Kroupa P., Pflamm-Altenburg J., 2015, *The Astrophysical Journal*, 810, 47
- Kapahi V. K., 1987, in Hewitt A., Burbidge G., Fang L. Z., eds, IAU Symposium Vol. 124, *Observational Cosmology*. pp 251–265
- Kellermann K. I., 1993, *Nature*, **361**, 134
- Kodama H., Sasaki M., 1984, *Progress of Theoretical Physics Supplement*, **78**, 1
- Krishnan C., Raju A., 2017, *Modern Physics Letters A*, **32**, 1750077
- Kroupa P., 2012, *Publ. Astron. Soc. Australia*, **29**, 395
- Kroupa P., 2015, *Canadian Journal of Physics*, **93**, 169
- Kroupa P., et al., 2010, *A&A*, **523**, A32
- Laviolette P. A., 1986, *ApJ*, **301**, 544
- Lerner E. J., 2006, in Lerner E. J., Almeida J. B., eds, American Institute of Physics Conference Series Vol. 822, First Crisis in Cosmology Conference. pp 60–74 (arXiv:astro-ph/0509611), doi:10.1063/1.2189123
- Lerner E. J., 2018, *MNRAS*, **477**, 3185
- Lerner E. J., Falomo R., Scarpa R., 2014, *International Journal of Modern Physics D*, **23**, 1450058
- López-Corredoira M., 2010, *International Journal of Modern Physics D*, **19**, 245
- Lubin L. M., Sandage A., 2001, *AJ*, **122**, 1084
- Marosi L. A., 2013, *Advances in Astronomy*, 2013, 917104
- Melia F., López-Corredoira M., 2018, *A&A*, **610**, A87
- Melia F., Shevchuk A. S. H., 2012, *MNRAS*, **419**, 2579
- Mo H. J., Mao S., White S. D. M., 1998, *MNRAS*, **295**, 319
- Mukhanov V. F., 2005, *Physical foundations of cosmology*. Cambridge Univ. Press, Cambridge
- Mukhanov V. F., Feldman H. A., Brandenberger R. H., 1992, *Phys. Rep.*, **215**, 203
- Noll S., et al., 2009, *A&A*, **499**, 69
- Pashchenko I. N., Vitrichchak V. M., 2011, *Astronomy Reports*, **55**, 293
- Peebles P. J. E., Nusser A., 2010, *Nature*, **465**, 565
- Planck Collaboration et al., 2016, *A&A*, **594**, A13
- Rassat A., Refregier A., 2012, *A&A*, **540**, A115
- Ribas I., Jordi C., Vilardell F., Fitzpatrick E. L., Hilditch R. W., Guinan E. F., 2005, *ApJ*, **635**, L37
- Riess A. G., Casertano S., Yuan W., Macri L. M., Scolnic D., 2019, arXiv e-prints, p. arXiv:1903.07603
- Schade D., Barrientos L. F., López-Cruz O., 1997, *ApJ*, **477**, L17
- Shen S., Mo H. J., White S. D. M., Blanton M. R., Kauffmann G., Voges W., Brinkmann J., Csabai I., 2003, *MNRAS*, **343**, 978
- Shenavar H., 2016, *Ap&SS*, **361**, 93
- Shenavar H., Javidan K., 2018, arXiv e-prints, p. arXiv:1810.05001
- Suess K. A., Kriek M., Price S. H., Barro G., 2019, arXiv e-prints, p. arXiv:1904.10992
- Trujillo I., et al., 2004, *ApJ*, **604**, 521
- Trujillo I., et al., 2006, *ApJ*, **650**, 18
- Trujillo I., Conselice C. J., Bundy K., Cooper M. C., Eisenhardt P., Ellis R. S., 2007, *MNRAS*, **382**, 109
- Vavrycuk V., 2017, *MNRAS*, **470**, L44
- Wei J.-J., Wu X.-F., Melia F., 2015, *MNRAS*, **447**, 479
- Wei J.-J., Melia F., Wu X.-F., 2017, *ApJ*, **835**, 270
- Weinberg S., 2008, *Cosmology*. OUP, Great Clarendon Street, Oxford OX2 6DP
- Wiklind T., Dickinson M., Ferguson H. C., Giavalisco M., Mobasher B., Grogin N. A., Panagia N., 2008, *ApJ*, **676**, 781
- Yennapureddy M. K., Melia F., 2017, *Journal of Cosmology and Astroparticle Physics*, 2017, 029
- Zhu Z.-H., Fujimoto M.-K., He X.-T., 2004, *A&A*, **417**, 833

## 8 APPENDIX

Cosmological perturbation theory is premised upon linear perturbation theory in curved spacetime. The linear perturbation theory consists of a background and a physical spacetime with a perturbation propagating on the background spacetime. The perturbation is seen as the difference between the pulled-back metric of the physical and the background metric, given as

$${}^l g_{\mu\nu} = \phi^*(g_{\mu\nu}) - {}^b g_{\mu\nu} \quad (17)$$

where  ${}^l g_{\mu\nu}$  denotes the perturbation,  $g_{\mu\nu}$  the physical metric,  ${}^b g_{\mu\nu}$  is the background metric and  $\phi^*$  is the pullback of the diffeomorphism  $\phi$ . The background spacetime is usually restricted to being a homogeneous and isotropic spacetime as perturbations on this spacetime can be written in terms of harmonic functions, which can be solved readily. Another reason is that on large scales the universe is homogeneous and isotropic.

Also we assume that the universe's departure from homogeneity and isotropy due to the perturbation is very small (Javanmardi et al. 2015; Javanmardi & Kroupa 2017). This enables us to take the Einstein tensor of the physical metric upto the first order of the linearized theory. This is valid as we assumed a weak gravitational field implying that the perturbation is small. For the background metric we use the flat FLWR metric with its components given as

$$\begin{aligned} {}^b g_{00} &= -1, \\ {}^b g_{ii} &= R^2(t), \end{aligned} \quad (18)$$

where  $R$  is the scale factor as a function of coordinate time  $t$ , and local perturbations can be decomposed into scalars, vectors, and tensors based on their transformation properties under 3D rotations. Further we take only the scalar perturbation as it takes prominence on cosmological scales over the vector and tensor perturbations since they characterise the energy density of inhomogeneities, which may play a role in formation of structure in the universe. The vector contribution represents rotation by the cosmological fluid which decays very quickly, thus not contributing on the cosmological scale. The tensor contributions manifest the gravitational waves which does not induce any perturbations on the perfect fluid in linear approximation (Mukhanov 2005). Therefore the local perturbation metric parametrised with scalar fields  $\Phi$  and  $\Psi$  under longitudinal (Newtonian) gauge is given as

$$\begin{aligned} {}^l g_{00} &= -2\Phi, \\ {}^l g_{ii} &= -2\Psi. \end{aligned} \quad (19)$$

For a derivation of the above equations in this gauge we refer to chapter 7 in Mukhanov (2005). For a review on different gauges in cosmological perturbation theory see chapter 4 in Bertschinger (1995), and for a good introduction to cosmological perturbation theory with a more general perturbation we refer to Bardeen (1980), Mukhanov, Feldman & Brandenberger (1992), Kodama & Sasaki (1984).

The Christoffel's symbols of the physical metric upto the first order are given as (Weinberg 2008)

$$\begin{aligned} {}^b \Gamma_{ij}^0 &= RR' \delta_{ij}, \\ {}^b \Gamma_{0j}^i &= {}^b \Gamma_{j0}^i = H \delta_{ij}, \end{aligned} \quad (20)$$

and for the local perturbation as (Shenavar 2016)

$$\begin{aligned} {}^l \Gamma_{00}^i &= \frac{\partial_i \Phi}{R^2}, \\ {}^l \Gamma_{i0}^0 &= \partial_i \Phi, \\ {}^l \Gamma_{ij}^0 &= -\delta_{ij}(2RR' \Phi + \Psi'), \\ {}^l \Gamma_{j0}^i &= \frac{\delta_{ij}}{R^2}(2H\Psi - \Psi'), \\ {}^l \Gamma_{jk}^i &= \frac{1}{R^2}(\delta_{jk}\partial_i \Psi - \delta_{ij}\partial_k \Psi - \delta_{ik}\partial_j \Psi). \end{aligned} \quad (21)$$

For the sake of brevity we will not explicitly write the Ricci tensor and Riemann tensor. For a detailed review on them refer to Bardeen (1980) and Shenavar (2016). The components of the background Einstein's tensor (Mukhanov 2005) are

$$\begin{aligned} {}^b G_{00} &= 3H^2, \\ {}^b G_{ij} &= (2H' + H^2)\delta_{ij}, \end{aligned} \quad (22)$$

and the components of the local Einstein's tensors are (Shenavar

2016)

$$\begin{aligned} {}^l G_{00} &= \frac{2}{R^4}(6\Phi R'^2 + \nabla^2 \Psi - 3RR'\Psi'), \\ {}^l G_{0j} &= \frac{R'}{R}\partial_j \Phi - \frac{R'}{R^3}4\partial_j \Psi + \frac{2}{R^2}\partial_j \Psi', \end{aligned} \quad (23)$$

$$\begin{aligned} {}^l G_{ij} &= (\delta_{ij}\nabla^2 - \partial_i\partial_j)\left(\Phi - \frac{\Psi}{R^2}\right) + 2\delta_{ij}\Psi'^2 + 2\delta_{ij}RR'\Phi' \\ &\quad + 4\delta_{ij}RR''\Phi + 2\delta_{ij}R'^2\Phi - 2\delta_{ij}\frac{R'}{R}\left(\Psi' - \frac{R'}{R}\Psi\right). \end{aligned} \quad (24)$$

The primes on the top of the symbols represent coordinate time derivatives. The rotational and translational invariance of the unperturbed energy-momentum tensor requires it to be a perfect fluid (Weinberg 2008), and for the perturbed metric we assume a general energy-momentum tensor. To establish a relationship between the two scalar fields we take off-diagonal elements of Eq. 24 and set the anisotropic inertia terms of the perturbed energy-momentum tensor to zero,

$$\partial_i\partial_j\left(\Phi - \frac{\Psi}{R^2}\right) = 0. \quad (25)$$

This is the famous result of cosmological perturbation theory in longitudinal (Newtonian) gauge. We refer the reader to Weinberg (2008) eq. 5.3.20, and Mukhanov (2005) eq. 7.46 for a detailed derivation of Eq.25 in longitudinal (Newtonian) gauge. We obtain a similar result for a static perturbation theory in Minkowski background metric with transverse gauge (generalisation of the longitudinal gauge) in eq. 7.56 of Carroll (2014).

Now to solve Eq. 25, we first fix the boundary conditions. Here we have four different boundary conditions: the Dirichlet B.C. where the function is fixed at the boundary, the Neumann B.C. where the normal derivative of the functions is fixed at the boundary, the Cauchy B.C. where the function and its normal derivative is fixed at the boundary, and lastly the Mixed B.C, e.g. a Dirichlet B.C. on the northern hemisphere and Neumann B.C. in the southern hemisphere.

For our case we will use the Neumann B.C. since the gravitational force is zero at the boundary (Shenavar 2016) and the Cauchy B.C. removes interesting dynamics from the system that we would like to study (Krishnan & Raju 2017) while the Mixed B.C. does not agree with our fundamental assumption of spacetime isotropy. The Dirichlet B.C. is the usually preferred solution in the literature, however the Neumann B.C. is equally stable on a closed surface, see chapter 9 in Arfken (2005). Therefore solving Eq.25 using the Neumann B.C. we obtain the solution as

$$\Phi = \frac{\Psi}{R^2} + c_1. \quad (26)$$

The general solution to Eq. 25 using the Neumann B.C. is

$$\Phi - \frac{\Psi}{R^2} = A_1(t, x) + A_2(t, y) + A_3(t, z) + c_1, \quad (27)$$

where the homogeneity and isotropy of the perturbations set the first three terms to zero yielding Eq. 26. The constant  $c_1$  is the spatial average of the perturbations, setting it to zero is equivalent to considering the Dirichlet B.C. (Mukhanov et al. 1992). Through out this paper we will use the Neumann B.C. with the solution given by Eq. 26. The interpretation for the constant  $c_1$  is still an open question. For an experimental determination of the value of  $c_1$  using strong lensing systems see Shenavar (2016).



This paper has been typeset from a  $\text{\TeX/L\AA\TeX}$  file prepared by the author.